Original Article

DOI: 10.5582/ddt.2026.01045

Duzhong Fang (DZF) alleviates rotenone-induced Parkinson's disease-like pathological alterations through regulation of the gut-brain axis *via* the intestinal TPH1/5-HT pathway

LiLi Li[1], Anran Lv[2], Jibao Yang[1], Xiran Li[1], Zishu Yan[1], Ziyi Zhong[1], Wenqing Tian[1], Bin Jia[1], Yanjun Zhang[3,4], Pengwei Zhuang[3,4,*], Hong Guo[1,*]

[1] State Key Laboratory of Component-based Chinese Medicine, Tianjin University of Traditional Chinese Medicine, Tianjin, China;
[2] School of Medical Technology, Tianjin University of Traditional Chinese Medicine, Tianjin, China;
[3] First Teaching Hospital of Tianjin University of Traditional Chinese Medicine, Tianjin, China;
[4] National Clinical Research Center for Chinese Medicine, Tianjin, China.

SUMMARY: The gut-brain axis is increasingly recognized as a critical pathway in Parkinson's disease (PD), but the gut-targeted mechanisms underlying the therapeutic effects of herbal formulas remain poorly understood. In this study, an enterogenic PD-like mouse model was established by long-term rotenone gavage and treated with Duzhong Fang (DZF) to investigate whether DZF acts through intestinally retained components to influence gut-brain α-synuclein pathology. DZF markedly improved motor dysfunction, increased nigral tyrosine hydroxylase (TH)-positive cell density, alleviated colonic inflammation, and reduced α-Syn accumulation in the vagus nerve and brain, while colonic α-Syn showed a decreasing trend. Mechanistically, DZF downregulated colonic TPH1 and 5-HT3A expression, reshaped gut microbiota composition, and modulated fecal metabolites related to tryptophan metabolism and the 5-HT biosynthetic pathway. Molecular docking predicted potential interactions between TPH1 and gut-retained gingerol-related compounds, including 6-shogaol, 10-gingerdione, 10-gingerol, and 4-gingerol. These findings suggest that DZF ameliorates rotenone-induced PD-like phenotypes and may act by modulating the intestinal TPH1/5-HT-related pathway and α-Syn pathology along the gut-brain axis. This study supports a gut-targeted, neural-regulated therapeutic paradigm for traditional Chinese medicine and provides potential lead compounds for gut-directed anti-PD intervention.

Keywords: Duzhong Fang, Parkinson's disease, gut-brain axis, α-synuclein

1. Introduction

Parkinson's disease (PD) is the second most common neurodegenerative disorder worldwide. Its main pathological features include progressive loss of dopaminergic neurons in the substantia nigra pars compacta of the midbrain and abnormal aggregation of α-synuclein (α-Syn) (*1*). Clinically, in addition to motor symptoms such as resting tremor, bradykinesia, rigidity, and postural instability, patients often present with non-motor symptoms, including hyposmia, depression, constipation, and gastrointestinal dysfunction (*2*). More importantly, by the time typical motor symptoms emerge, more than 50% of dopaminergic neurons in the substantia nigra have already been lost, indicating that the disease has reached an irreversible stage (*3*). Therefore, investigating the early origin of PD and developing etiology-targeted intervention strategies have become central scientific challenges in the field.

Accumulating evidence suggests that pathological changes in PD may originate outside the central nervous system (*4*). Among these, gastrointestinal dysfunction, as one of the most common and earliest non-motor symptoms of PD, can precede motor symptoms by several years or even more than a decade (*5*). Prospective cohort studies have confirmed that functional gastrointestinal disorders, such as constipation, are associated with a significantly increased risk of developing PD (*6*). These findings strongly support the hypothesis that the gut may be the initial site of PD pathogenesis (*4,7*). Therefore, elucidating the gut-brain connection is of critical importance for developing early intervention strategies for PD.

In 2003, based on a systematic pathological analysis of autopsy specimens from patients with sporadic PD, Braak and colleagues first proposed that pathological

α-synuclein (α-Syn) appears initially in the dorsal motor nucleus of the vagus nerve and the enteric nervous system, and then propagates retrogradely along neuroanatomical pathways to the substantia nigra of the midbrain (*4*). This seminal work formally established the "gut-origin hypothesis" of PD. Subsequently, numerous studies have confirmed that pathogenic α-Syn is not only present in the midbrain substantia nigra, but is also widely distributed in other brain regions, the spinal cord, the gastrointestinal tract, and even the blood, where it acts as an initiating factor in early PD pathogenesis (*8,9*). Experimental evidence further demonstrates that injection of α-Syn preformed fibrils into the gut of animal models induces the propagation of this protein along the vagus nerve to the brainstem, leading to damage of dopaminergic neurons (*7,9,10*). Notably, pathogenic α-Syn is predominantly enriched in enteric neurons under inflammatory conditions, and its expression level positively correlates with the severity of tissue inflammation (*11*). Collectively, these findings suggest that the intestinal inflammatory microenvironment is a key driver triggering local abnormal α-Syn aggregation in the gut.

During the initiation and progression of intestinal inflammation, dysregulation of the gut microbiota and its metabolites play a central regulatory role (*12*). In recent years, the critical role of the gut microbiota as a key modulator of gut-brain signaling has become increasingly recognized, giving rise to the concept of the "microbiota-gut-brain axis" (*13*). Accumulating evidence indicates that the gut microbiota contributes importantly to PD through this axis (*14*). Patients with PD commonly exhibit structural dysbiosis, characterized by an increase in opportunistic pathogens and a decrease in short-chain fatty acid-producing bacteria. These microbial alterations are closely correlated with the severity of motor symptoms and the burden of non-motor symptoms (*15*). Dysbiosis not only disrupts the integrity of the intestinal epithelial barrier and exacerbates local inflammatory responses but also influences host neuroendocrine functions by modulating pathways such as tryptophan metabolism (*16*). Intervention studies targeting the microbiota using antibiotics, probiotics, or fecal microbiota transplantation have confirmed a causal relationship between the gut microbiota and PD, and have demonstrated beneficial effects on host health (*17-22*). Bidirectional communication between the nervous system and the gastrointestinal tract is achieved through multiple pathways, including the vagus nerve, the immune system, and bacterial metabolites (*23*). Therefore, targeting the gut microbiota and its metabolic network represents a promising strategy for early intervention in PD.

Duzhong Fang (DZF) is composed of *Eucommia ulmoides* Oliv. (Duzhong), *Dendrobium nobile* Lindl. (Shihu), *Rehmannia glutinosa* Libosch. (Dihuang), and *Zingiber officinale* Roscoe (Ganjiang). Our previous studies have shown that DZF significantly improves motor coordination and protects dopaminergic-related markers in acute and chronic mouse models of PD (*24,25*). Notably, while some components of DZF can enter the brain, others persist in fecal matter and intestinal contents as parent compounds (*e.g.*, 4-, 6-, 8-, and 10-gingerol; 6-shogaol; 10-gingerdione; scopoletin; pyroglutamic acid; cinnamic acid; and palmitoleic acid), exhibiting distinct intestinal-retention characteristics (*26*). This finding suggests that the effects of DZF may not rely solely on direct entry into the central nervous system but may also involve modulation of gut-related pathways. To test this hypothesis, the present study employed a low-dose rotenone oral gavage-induced gut-origin PD-like mouse model. We aimed to investigate whether DZF ameliorates established PD-like motor and pathological phenotypes through gut-related mechanisms, thereby providing experimental evidence for gut-targeted intervention in PD.

2. Materials and Methods

2.1. Experimental animals and drugs

Male SPF C57BL/6J mice, aged 8 weeks and weighing 23-25 g, were obtained from Beijing Weitong Lihua Biotechnology Co., Ltd. (License No.: SCXK (Jing) 2019-0008). All experimental procedures were approved by the Animal Ethics Committee of Tianjin University of Traditional Chinese Medicine (Approval No. TCM-LAEC2020084).

To establish the enterogenic PD-like model, 40 mice were randomly divided into four groups: Control, 1 M, 3 M, and 5 M (n = 10 per group). According to Pan-Montojo *et al.* (*27*), mice in the 1 M, 3 M, and 5 M groups were administered rotenone (5 mg/kg; 0.1mL/10g) by daily gavage for 1, 3, or 5 consecutive months, respectively. The Control group received the same volume of vehicle (1% sodium carboxymethyl cellulose containing 1.25% chloroform), underwent the same handling procedures.

To evaluate the effects of DZF on established PD-like phenotypes, 30 mice were randomly divided into control, model, and DZF groups (n = 10 per group). Mice in the model and DZF groups received rotenone (5 mg/kg; 0.1 mL/10g) daily by gavage, whereas the control group received the same volume of vehicle (1% sodium carboxymethyl cellulose containing 1.25% chloroform). Rotenone or vehicle administration continued throughout the 8-month experimental period. Beginning in month 6, after completion of 5 months of rotenone exposure, mice in the DZF group additionally received DZF extract (20 g crude drug/kg; 0.1mL/10g) by gavage 1 h after rotenone administration; control and model mice received an equal volume of normal saline. The dosage of DZF was based on our previous study (*25*).

Duzhong Fang (DZF) was prepared according to the

proportional composition described in Bei Ji Qian Jin Yao Fang (Essential Prescriptions Worth a Thousand Pieces of Gold for Emergency). For experimental preparation, the herbal materials were scaled according to this proportional relationship as follows: *Eucommia ulmoides* (1,000 g), *Dendrobium nobile* (10 g), *Zingiber officinale* (15 g), and *Rehmannia glutinosa* (15 g). These amounts represent scaled experimental quantities rather than the original dosages described in the classical text. The crude herbal materials were mixed and processed for subsequent experiments. The administered crude drug dose was calculated according to the proportional relationship of the experimental formulation. The herbs were reflux-extracted twice with 75% ethanol, first with 10 volumes for 2 h and then with 8 volumes for 2 h. The two extracts were combined, concentrated under reduced pressure, aliquoted, and stored at − 20°C. Before administration, the concentrated extract was diluted with distilled water to the required concentration, corresponding to a dose of 20 g crude drug/kg. The preparation procedure was consistent with our previously reported DZF preparation and chemical characterization (*26*).

2.2. Behavioral tests

Behavioral tests were performed according to previously described methods (*25*). Mice were subjected to behavioral training for three days prior to the formal experiment. During the formal test, each mouse was tested three times, and the average value was used for statistical analysis.

2.3. Immunohistochemistry (IHC) staining

Mice were perfused transcardially, and the brain, colon, and vagus nerve were collected, fixed in 4% paraformaldehyde, embedded in paraffin, and sectioned. Following deparaffinization and rehydration, sections were treated with 3% H_2O_2 to quench endogenous peroxidase activity. Antigen retrieval was performed in sodium citrate buffer, and sections were blocked with goat serum. The sections were incubated overnight at 4°C with primary antibodies against tyrosine hydroxylase (TH) (rabbit, Proteintech, 1:500) and α-Syn (rabbit, Abcam, 1:200). The next day, sections were incubated with goat anti-rabbit IgG secondary antibody for 1 h at 37°C. After DAB visualization, images were captured under a light microscope. TH-positive cells in the substantia nigra pars compacta were counted, and α-Syn expression in the brain, vagus nerve, and colon was analyzed.

2.4. Immunofluorescence (IF) staining

Brain and colon sections were permeabilized with 0.03% Triton X-100 and blocked with 10% donkey serum for 1 h at room temperature. Sections were incubated overnight at 4°C with primary antibodies against α-Syn (goat, Abcam, 1:400), TPH1 (rabbit, Affinity, 1:200), 5-HT3A (rabbit, Affinity, 1:200). After washing, sections were incubated for 1 h at room temperature with corresponding secondary antibodies. Nuclei were counterstained with DAPI. Sections were mounted with anti-fade mounting medium and imaged under a fluorescence microscope (Nikon, Japan). Images were analyzed using NIS Elements software (Nikon).

2.5. Hematoxylin and eosin (H&E) staining

Colon tissue samples were collected and fixed in 4% formaldehyde solution. After fixation, the tissues were rinsed under running tap water for 24 h, dehydrated through a graded ethanol series (70%, 80%, 95%, and absolute ethanol), cleared in xylene, and embedded in paraffin. Sections were cut at a thickness of approximately 5 μm, baked at 73°C to enhance adhesion, and then stained with H&E. Histopathological changes in the colon were observed and compared among experimental groups under a light microscope.

2.6. Western blotting

Colon tissues were collected from euthanized mice and weighed. Proteins were extracted by homogenizing the tissues in RIPA lysis buffer (10 μL per mg of tissue) on ice. The homogenate was centrifuged at 15,000 rpm for 10 min at 4°C, and the supernatant was collected for protein quantification using the BCA method. Equal amounts of protein were separated by SDS-PAGE and transferred onto PVDF membranes. The membranes were blocked with 5% skim milk in TBST for 1 h at room temperature, followed by overnight incubation at 4°C with primary antibodies against β-actin (proteintech, 66009-1-Ig, 1:1,000), Clathrin (abcam, ab21679, 1:1,000), IL-1β (Abcam, ab234437, 1:1,000), IL-6 (Abcam, ab290735, 1:1,000), TNF-α (Abcam, ab183218, 1:1,000), and IL-10 (Abcam, ab9969, 1:1,000). After washing, the membranes were incubated with HRP-conjugated goat anti-rabbit or anti-mouse secondary antibodies (Beyotime, a0208, a0216, 1:1,000) for 1 h at room temperature. Protein bands were visualized using a chemiluminescence imaging system, and band intensities were quantified using ImageJ software for statistical analysis.

2.7. Quantitative real-time PCR (qRT-PCR) analysis

Total RNA was extracted from fresh colon tissues using the Eastep™ Super Total RNA Extraction Kit (LS1040, Promega, China) according to the manufacturer's instructions. Briefly, freshly collected colon tissues were homogenized in RNA lysis buffer, and the lysates were processed through silica membrane-based spin

columns. After DNase I treatment to remove genomic DNA contamination, purified RNA was eluted with nuclease-free water. The concentration and purity of RNA were determined using a spectrophotometer, and qualified RNA samples were used for subsequent reverse transcription.

Complementary DNA (cDNA) was synthesized using the GoScript™ Reverse Transcription Mix (A2790, Promega, China) according to the manufacturer's protocol. Quantitative real-time PCR was performed using the SuperReal PreMix Plus (SYBR Green) (FP205-02, Tiangen Biotech, China) on a CFX Connect Real-Time PCR Detection System (Bio-Rad Laboratories, Singapore). The amplification conditions were as follows: initial denaturation at 95°C for 15 min, followed by 40 cycles of denaturation at 95°C for 10 s and annealing/extension at 60°C for 32 s.

The expression levels of target genes were normalized to the endogenous reference gene β-actin. Relative gene expression levels were calculated using the $2^{-\Delta\Delta Ct}$ method. The primer sequences used for qRT-PCR analysis are listed in Table 1.

2.8. 16S rRNA gene sequencing

Total genomic DNA was extracted from fecal samples using the CTAB/SDS method, and its purity and concentration were determined. The V3–V4 hypervariable region of the 16S rRNA gene was amplified by PCR using barcoded specific primers and a high-fidelity DNA polymerase. PCR products were separated by electrophoresis on a 2% agarose gel, and the target bands were excised and purified using the AxyPrep DNA Gel Extraction Kit (Axygen Biosciences, Union City, CA, USA). Purified amplicons were initially quantified by agarose gel electrophoresis and subsequently accurately quantified using the QuantiFluor™-ST Blue Fluorescence Quantitation System (Promega Corporation, Madison, WI, USA). Based on the required sequencing depth, purified products were pooled in equimolar ratios, and sequencing libraries were constructed using the New England Biolabs (NEB, Ipswich, MA, USA). Library quality was assessed using the Agilent 2100 Bioanalyzer and the Qubit system, and only qualified libraries were subjected to sequencing.

After sequencing, microbial community composition was analyzed based on taxonomic annotation. Differential microbial taxa between the model and DZF groups were identified by comparing genus-level relative abundances using Welch's *t*-test implemented in STAMP software. Significantly altered bacterial genera were determined based on differences in mean relative abundance, 95% confidence intervals, and corresponding *P* values. Spearman correlation analysis was performed to evaluate the associations between differential bacterial genera and tryptophan-related metabolites. Correlation coefficients (*r*) and corresponding *P* values were calculated.

Table 1. Primer sequences for RT-qPCR analysis

Gene Name	Primer Sequence	
β-actin	forward	GTGCTATGTTGCTCTAGACTTCG
	reverse	ATGCCACAGGATTCCATACC
Tph1	forward	TCCGTCCTGTGGCTGGTTACC
	reverse	AGGTGTCTGGCTCTGGAGTGTAG

2.9. Untargeted metabolomics analysis

Fresh fecal samples were collected from mice and homogenized with ice-cold methanol-acetonitrile-water (2:2:1). The mixture was vortexed, ultrasonicated at low temperature for 30 min, and then incubated at − 20°C for 10 min. After centrifugation at 14,000 g for 20 min at 4°C, the supernatant was collected and vacuum-dried. The dried extract was reconstituted in acetonitrile-water (1:1), vortexed, and centrifuged again at 14,000 g for 15 min at 4°C. The resulting supernatant was analyzed using ultra-high performance liquid chromatography coupled with Q Exactive mass spectrometry (UHPLC-Q Exactive MS) for data acquisition.

2.10. Molecular docking

The three-dimensional structures of the intestinally retained DZF components identified in our previous study were obtained from the PubChem database, including 6-shogaol (CID: 5281794), 10-gingerdione (CID: 5317591), 10-gingerol (CID: 168115), 4-gingerol (CID: 5317596), 6-gingerol (CID: 442793), 8-gingerol (CID: 168114), cinnamic acid (CID: 444539), palmitoleic acid (CID: 445638), pyroglutamic acid (CID: 7405), scopoletin (CID: 5280460).

The crystal structure of human tryptophan hydroxylase 1 (TPH1) was retrieved from the RCSB Protein Data Bank (PDB ID: 8CJK; UniProt accession: P17752; *https://www.rcsb.org/*). Molecular docking simulations were performed using AutoDock Tools (version 1.5.6; *https://autodock.scripps.edu/*). The binding affinity of each ligand with TPH1 was evaluated based on the predicted binding energy. Docking conformations with favorable binding energies were selected for visualization. The interaction modes between TPH1 and representative compounds were visualized using PyMOL (*https://pymol.org/2/*). The ligand structures were energy minimized before docking.

2.10. Statistical analysis

Continuous data are presented as mean ± standard error of the mean (SEM). Comparisons between two groups were performed using an unpaired *t*-test, and comparisons among multiple groups were conducted

using one-way analysis of variance followed by Tukey's post hoc test when the assumptions of parametric testing were satisfied. Ordinal outcomes, including colonic histopathological scores and traction-test scores, were analyzed using the Kruskal–Wallis test followed by Dunn's multiple-comparison test. $P < 0.05$ was considered statistically significant.

3. Results

3.1. Low-dose rotenone gavage for five months successfully establishes an enterogenic PD mouse model

To establish a gut-derived PD-like model, mice were administered rotenone (5 mg/kg) by gavage for 1, 3, or 5 months, while control mice received vehicle administration throughout the experimental period. H&E staining revealed progressive colonic damage in rotenone-treated mice, which was most pronounced after 5 months of rotenone exposure (Figure 1A-B). α-Syn expression in the colon, vagus nerve, and brain gradually increased with prolonged rotenone exposure and was significantly elevated after 5 months (Figure 1C-F). Motor-function assessment showed prolonged pole-test time, reduced grip strength, and decreased traction-test scores following rotenone exposure, with the most prominent impairments observed at 5 months (Figure 1G-I). Collectively, these findings indicate that 5 months of rotenone gavage established PD-like intestinal, pathological, and motor phenotypes in mice.

3.2. DZF ameliorates motor deficits and preserves TH-positive cell density in a gut-derived PD mouse model

After 5 months of low-dose rotenone exposure, mice exhibited PD-like pathological alterations and motor deficits. Therefore, DZF administration was initiated from month 6 onward while rotenone exposure was continuously maintained to evaluate its effects on established PD-like phenotypes. DZF treatment significantly improved motor performance, as evidenced by reduced pole-test descent time, increased rotarod latency, and amelioration of rotenone-induced gait abnormalities (Figure 2B-G). Consistent with the behavioral improvement, TH immunostaining showed that DZF attenuated the rotenone-induced reduction in TH-positive cell density in the substantia nigra (Figure 2H-I). These findings demonstrate that DZF exerts a protective effect against PD-like pathology in a gut-derived mouse model.

3.3. DZF attenuates intestinal pathology and inflammation in rotenone-induced PD mice

DZF not only ameliorated the behavioral deficits but also improved intestinal pathological alterations and the inflammatory microenvironment in rotenone-induced PD mice. As shown in Figure 3A-B, compared with the model group, DZF intervention improved intestinal injury, accompanied by a downward trend in the colonic pathological score. Western blot analysis further revealed that DZF treatment suppressed the aberrant elevation of pro-inflammatory cytokines IL-6, TNF-α and IL-1β in the colon of model mice, while restoring the expression level of the anti-inflammatory cytokine IL-10 to near normal (Figure 3C-G).

3.4. DZF alleviates α-Syn-related pathology along the gut-brain axis

Chronic intestinal inflammation has been associated with abnormal α-Syn accumulation in the gut and its involvement in gut-brain communication through the vagus nerve (*9*). We therefore examined α-Syn expression in the colon, vagus nerve, and brain (Figure 4A-C). Rotenone exposure markedly increased α-Syn accumulation in these tissues. Following DZF treatment, α-Syn expression was significantly decreased in the vagus nerve and brain, while a downward trend was observed in the colon (Figure 4D-F). These findings indicate that DZF effectively alleviates rotenone-induced α-Syn-associated pathological alterations along the gut-vagus-brain axis, suggesting a potential regulatory role of DZF in modulating α-Syn-related pathology.

3.5. DZF ameliorates gut microbiota dysbiosis in rotenone-induced PD mice

To further investigate the impact of DZF on the intestinal microenvironment, the composition and abundance of gut microbiota in fecal samples from each group were analyzed. A Venn diagram was used to illustrate the distribution of operational taxonomic units (OTUs) among the groups. As shown in Figure 5A, a total of 915 shared OTUs were identified among the control, model, and DZF groups, with 725, 41, and 201 unique OTUs in each group, respectively. Principal coordinate analysis (PCoA) based on unweighted UniFrac distance was performed to visualize the similarity of fecal microbiota structure in a reduced-dimensional space. The results in Figure 5B showed that samples with similar microbial composition clustered more closely, indicating that while certain similarities existed among groups, their microbiota structures were clearly distinguishable.

Further genus-level differential-abundance analysis (Figure 5C-D) identified 11 genera that differed between the DZF and model groups, including *Anaerotruncus*, *Devosia*, Family XIII AD3011 group, *Muribaculum*, *Parafrigoribacter*, and *Pedobacter*.

3.6. DZF modulates the gut microbiota-tryptophan metabolism axis in PD model mice

Given that DZF treatment significantly reshaped the

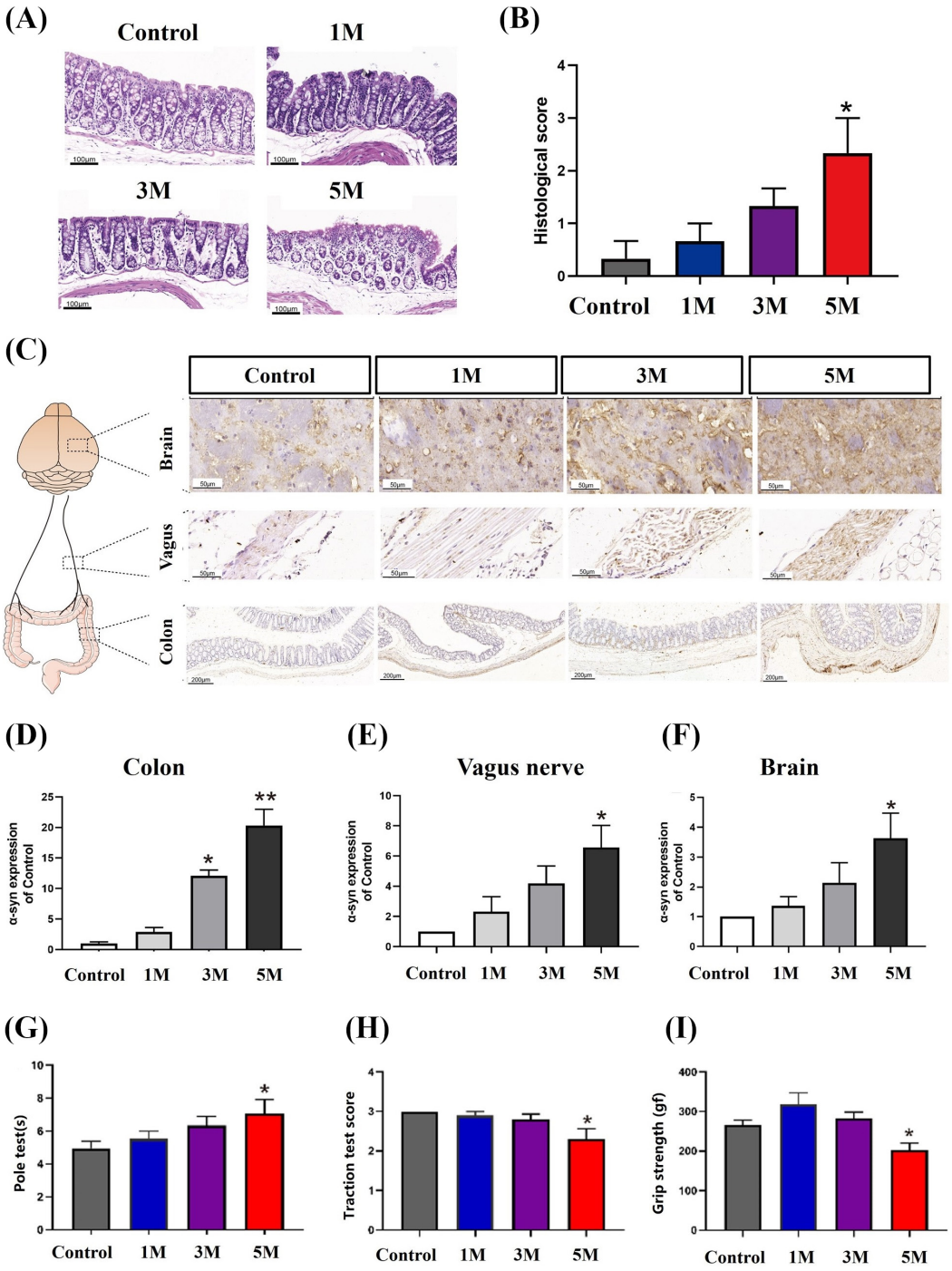

Figure 1. Rotenone treatment induces intestinal injury and motor dysfunction in mice after 5 months. Five months of rotenone treatment exacerbated intestinal tissue damage, as evidenced by structural abnormalities in H&E-stained colon sections (**A**) and increased histological injury scores (**B**). α-Syn expression increased in the colon, brain, and vagus nerve (**C-F**), accompanied by motor dysfunction characterized by impaired pole-test performance, reduced traction-test scores, and decreased grip strength (**G-I**). Data are presented as mean ± SEM. For (**A-F**), $n = 3$ per group; for (**G-I**), $n = 10$ per group. The traction test scores (**H**) were analyzed using the Kruskal–Wallis test followed by Dunn's multiple comparisons test. *$P < 0.05$ and **$P < 0.01$ compared with the control group.

gut microbiota composition, we further investigated whether these microbial alterations were accompanied by changes in intestinal metabolic profiles. Untargeted metabolomics was therefore performed to evaluate the effects of DZF on fecal metabolites in the rotenone-induced PD-like mouse model. The orthogonal partial least squares discriminant analysis (OPLS-DA) score plot demonstrated a clear separation between the DZF and model groups, indicating that DZF treatment altered the overall fecal metabolic profile (Figure 6A). KEGG pathway analysis revealed that tryptophan metabolism was significantly enriched and exhibited a relatively high pathway-impact value among the altered metabolic pathways (Figure 6B). Further analysis of

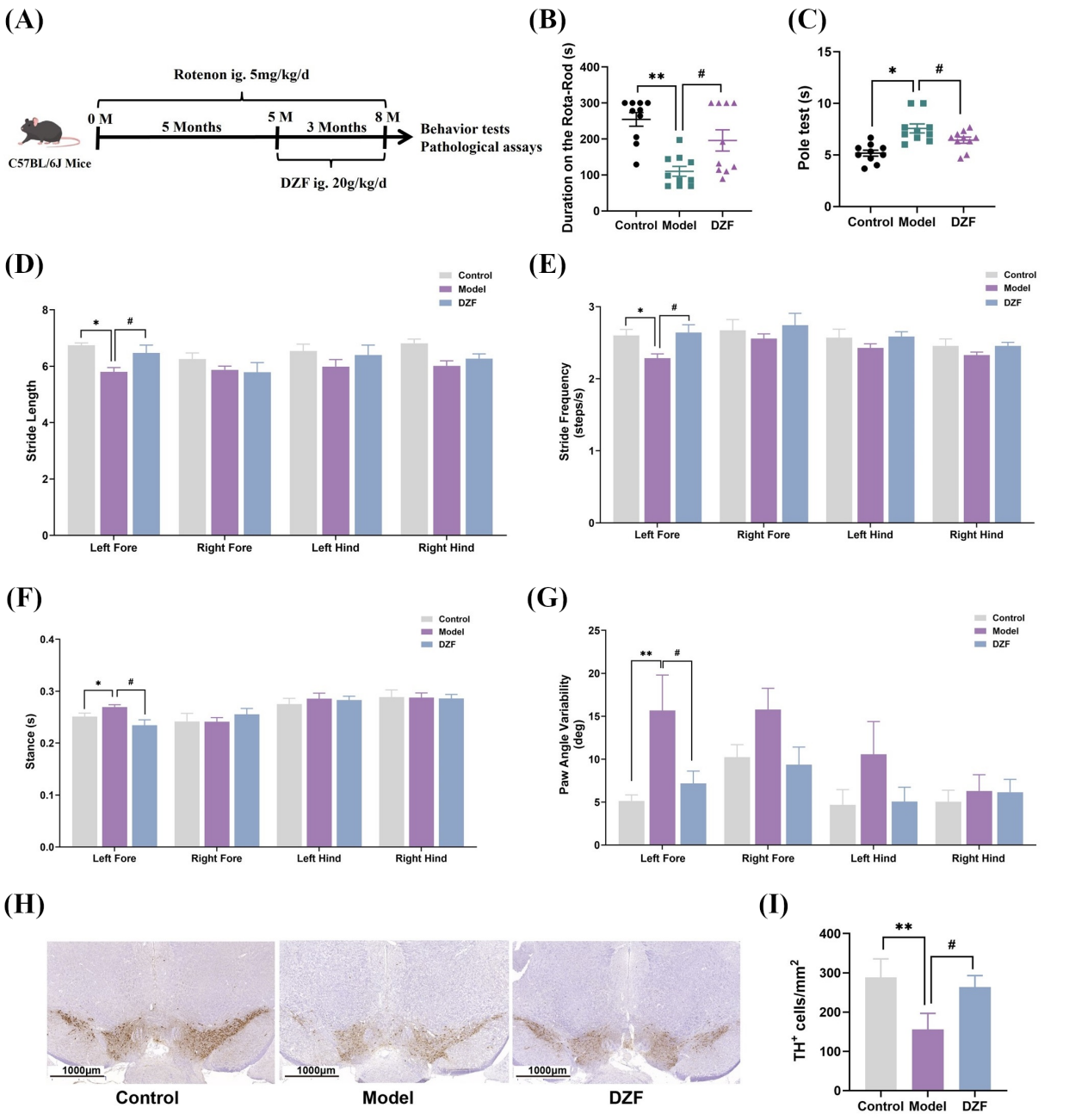

Figure 2. Effects of DZF on motor dysfunction and nigral TH immunoreactivity in rotenone-induced PD-like mice. (**A**) Experimental timeline showing that rotenone administration continued through month 8 and that DZF treatment began in month 6. DZF improved rotarod performance (**B**), pole-test performance (**C**), and gait parameters (**D-G**). DZF also attenuated the reduction in TH-positive cell density and TH immunoreactivity in the substantia nigra pars compacta (**H-I**). Data are presented as mean ± SEM. For (**B-G**), $n = 10$ per group; for (**H-I**), $n = 3$ per group. $^{*}P < 0.05$, $^{**}P < 0.01$ compared with the control group; $^{\#}P < 0.05$ compared with the model group.

tryptophan-related metabolites revealed alterations in L-tryptophan and 5-hydroxy-L-tryptophan (5-HTP), key intermediates involved in serotonin biosynthesis. These findings suggested a potential involvement of intestinal tryptophan metabolism in the effects of DZF and provided a basis for further investigation of TPH1/5-HT-related signaling (Figure 6C). Furthermore, Spearman correlation analysis demonstrated significant associations between differential bacterial genera and tryptophan-related metabolites. Notably, Pedobacter and Anaerotruncus showed significant correlations with these metabolites (Figure 6D). Collectively, these findings suggest that DZF-induced microbiota remodeling is associated with alterations in tryptophan-related metabolic profiles, highlighting a potential microbiota–metabolite interaction underlying the effects of DZF.

3.7. DZF modulates intestinal TPH1/5-HT-related signaling in rotenone-induced PD-like mice

Based on the alterations in tryptophan-related

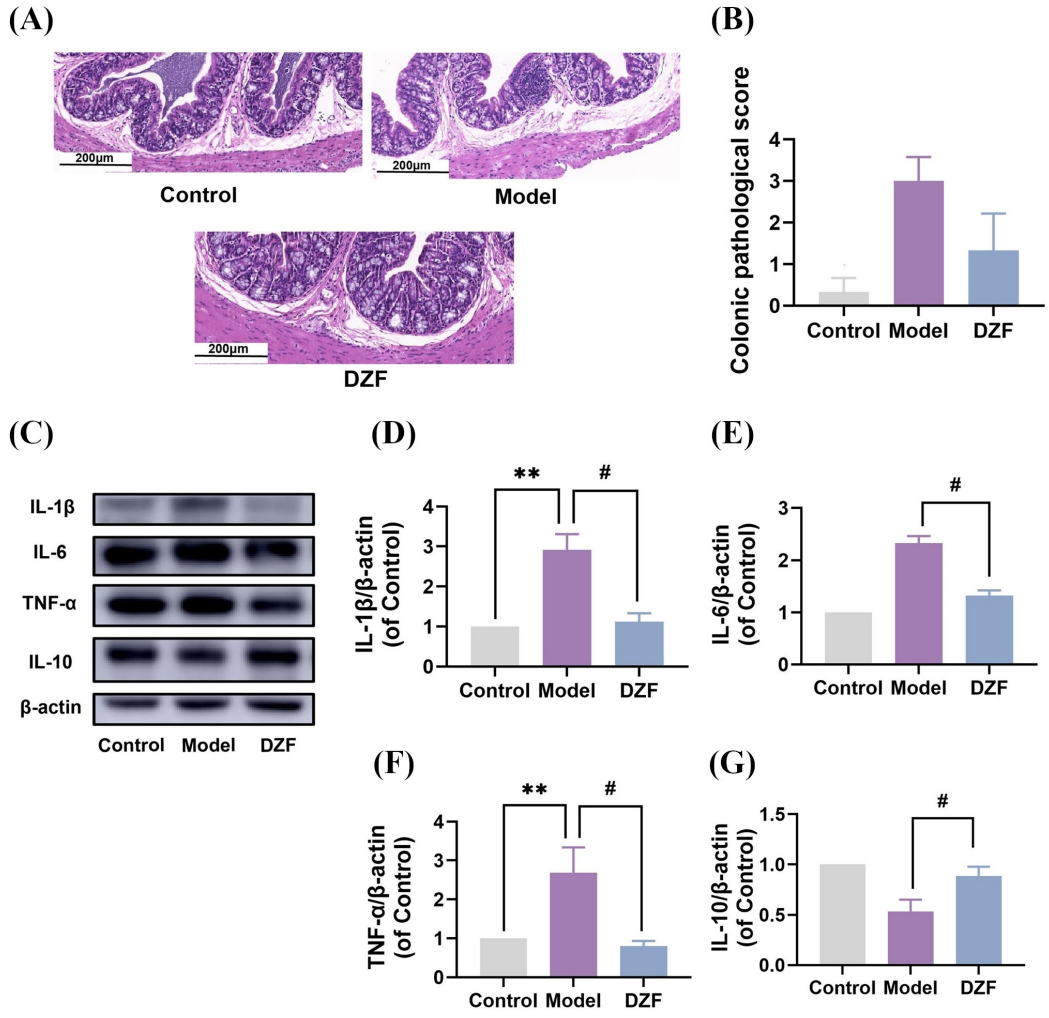

Figure 3. DZF ameliorates colonic histopathology and attenuates intestinal inflammation in PD mice. DZF treatment showed a tendency to alleviate colonic histopathological damage, as evaluated by H&E staining (**A**) and corresponding histological injury scores (**B**). Western blot analysis showed that DZF treatment modulated the colonic inflammatory microenvironment by decreasing the protein expression of pro-inflammatory cytokines, including IL-1β (**D**), IL-6 (**E**), and TNF-α (**F**), while upregulating the anti-inflammatory cytokine IL-10 (**G**). Representative western blot images are shown in (**C**). Data are presented as mean ± SEM, $n = 3$ per group. The colonic pathological scores (**B**) were analyzed using the Kruskal–Wallis test followed by Dunn's multiple comparisons test. $^{*}P < 0.05$, $^{**}P < 0.01$ compared with the control group; $^{\#}P < 0.05$ compared with the model group.

metabolites identified by metabolomics analysis, we further investigated whether DZF treatment affected intestinal TPH1/5-HT-related signaling. TPH1 is the rate-limiting enzyme responsible for converting L-tryptophan into 5-hydroxy-L-tryptophan (5-HTP), an intermediate precursor involved in 5-HT biosynthesis. Immunofluorescence staining showed that rotenone exposure significantly increased TPH1 fluorescence intensity in the colon, whereas DZF treatment markedly reduced TPH1 expression (Figure 7A-B). Similarly, the expression of the serotonin receptor 5-HT3A was elevated in the model group and decreased following DZF administration (Figure 7C-D). Consistently, qPCR analysis further demonstrated that intestinal TPH1 mRNA expression was increased after rotenone exposure and was attenuated by DZF treatment (Figure 7E). In addition, western blot analysis revealed that DZF treatment reduced the elevated expression of Clathrin induced by rotenone exposure (Figure 7F-G). Collectively, these findings suggest that DZF may regulate intestinal TPH1/5-HT-related signaling and associated intracellular transport processes in rotenone-induced PD-like mice.

3.8. Molecular docking predicts potential interactions between DZF components and TPH1

To further validate the mechanism of action of DZF, molecular docking analysis was performed between TPH1 and the intestinal active components of DZF identified in our previous study. Figure 8A presents a heatmap of the binding affinities of ten major intestinal active components of DZF with TPH1. Among them, 6-shogaol, 10-gingerdione, 10-gingerol, and 4-gingerol exhibited stable binding conformations and low binding energies with TPH1 (Figure 8B). These findings suggest

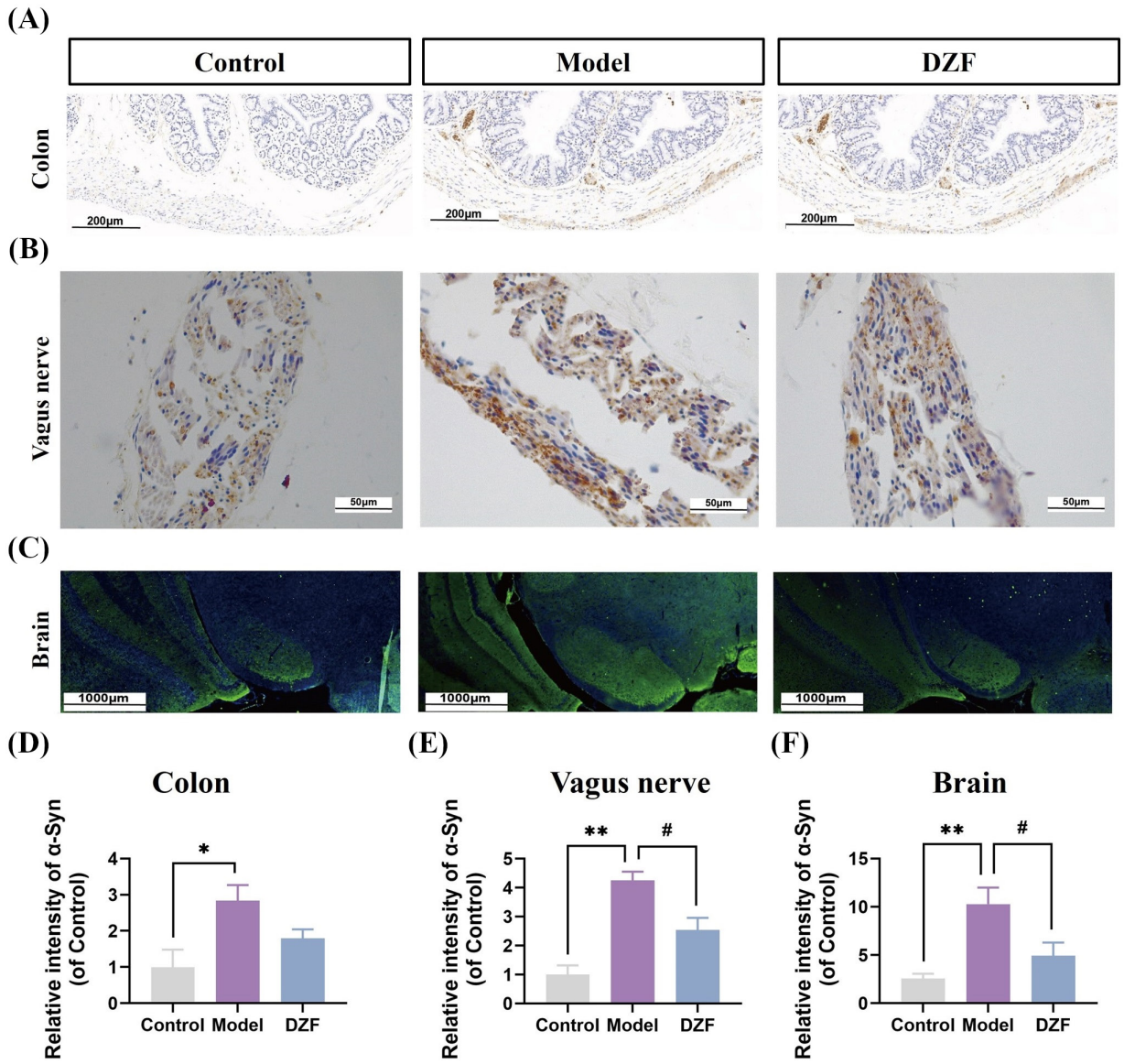

Figure 4. Effects of DZF on α-Syn-related pathology along the gut-brain axis. Representative immunohistochemical/immunofluorescence images and quantitative analyses show α-Syn expression in the colon (**A**, **D**), vagus nerve (**B**, **E**), and brain (**C**, **F**). DZF significantly reduced α-Syn expression in the vagus nerve and brain, whereas the reduction in the colon represented a non-significant downward trend. Data are presented as mean ± SEM, $n = 3$ per group. $^{*}P < 0.05$, $^{**}P < 0.01$ compared with the control group; $^{\#}P < 0.05$ compared with the model group.

that several intestinally active components of DZF may have potential interactions with TPH1, supporting the possible involvement of TPH1-related signaling in the biological effects of DZF.

4. Discussion

In recent years, the gut-brain axis has emerged as an important regulatory network in PD pathogenesis, linking intestinal homeostasis with central neurodegenerative changes (*28-30*). Within this framework, our findings indicate that DZF ameliorates established rotenone-induced PD-like phenotypes and may act by modulating the intestinal TPH1/5-HT-related pathway and α-Syn-related pathology along the gut-brain axis. These observations support further investigation of gut-targeted mechanisms underlying the effects of traditional Chinese medicine in PD models.

The low-dose rotenone gavage model employed in this study provides a unique experimental platform for investigating enterogenic PD. Unlike systemic neurotoxins, rotenone (5 mg/kg) is highly lipophilic and poorly absorbed from the gastrointestinal tract, allowing it to act preferentially on the gut without direct entry into the central nervous system (*27*). This rotenone induced enterogenic PD model has been widely used in related research (*31,32*). Based on this, we designed a gradient administration regimen of 1, 3, and 5 months. The results showed that after five months of gavage, the model mice exhibited sequential accumulation of pathological

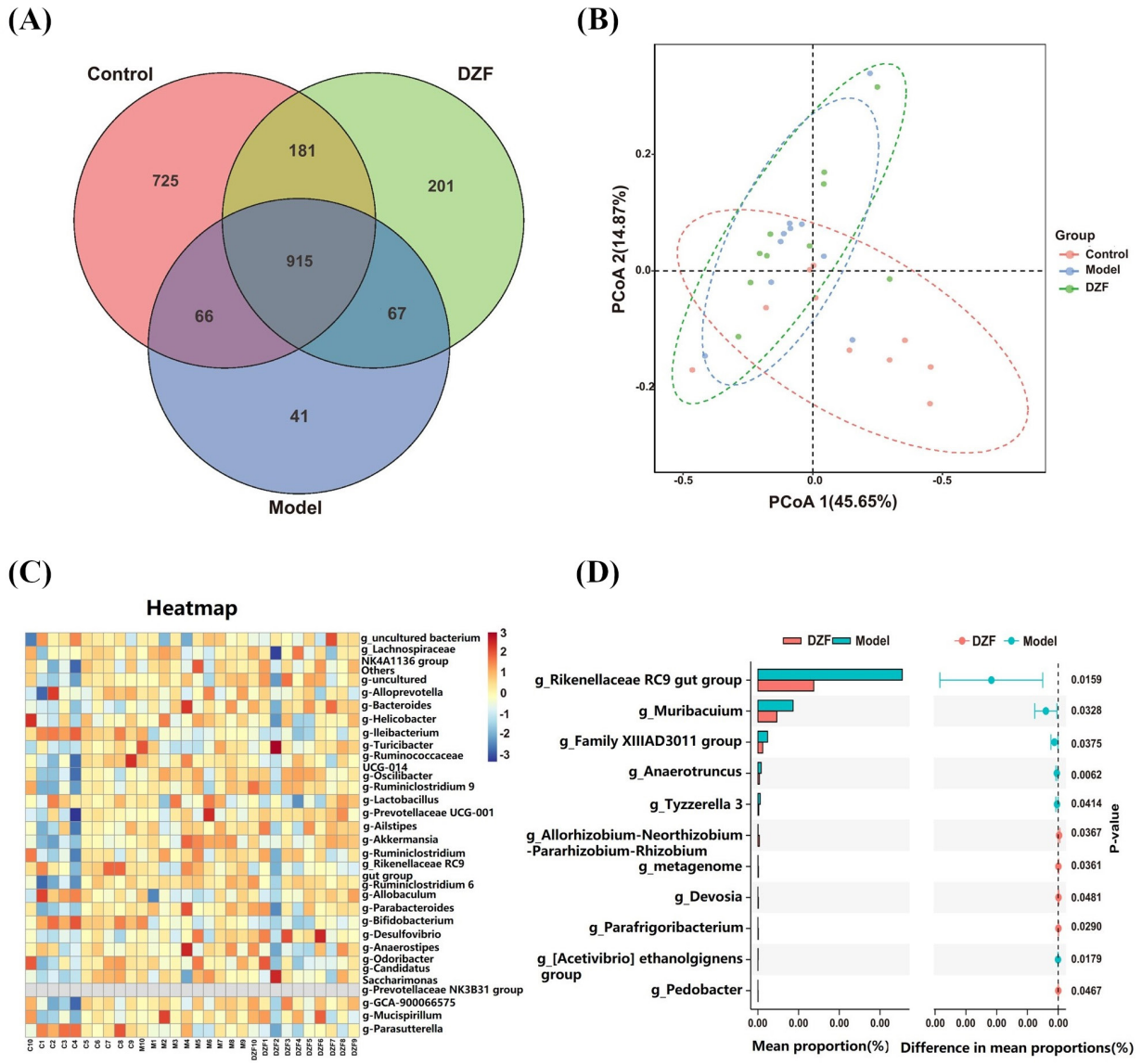

Figure 5. DZF intervention alters gut microbiota composition in PD-like mice. The Venn diagram (**A**) summarizes shared and unique OTUs among the control, model, and DZF groups. PCoA based on unweighted UniFrac distance (**B**) shows differences in microbial-community structure. The heatmap (**C**) and between-group genus-level differential-abundance analysis (**D**) identify genera that differ between the model and DZF groups; panel D presents mean relative abundance, the between-group difference, and the corresponding *P* value.

α-Syn in the colon, vagus nerve, and substantia nigra, accompanied by motor dysfunction, thereby faithfully recapitulating the temporal "gut→vagus→brain" pathological cascade. Importantly, this model closely replicates the "body first" PD subtype, which accounts for approximately 46% of patients presenting with early gastrointestinal dysfunction (*33*), providing an ideal animal platform for evaluating early intervention strategies targeting the gut.

In this study, low-dose rotenone gavage successfully induced PD-like phenotypes accompanied by pronounced intestinal microenvironment disturbances, including colonic inflammatory-cell infiltration, an imbalance in inflammatory cytokine profiles characterized by increased pro-inflammatory cytokines IL 1β, IL 6, and TNF α and decreased IL-10, as well as gut microbiota dysbiosis. These findings are consistent with those of Sampson *et al.* (*12*), who demonstrated that gut microbiota dysbiosis is necessary for motor deficits and neuroinflammation in PD models (*12*). Following DZF intervention, intestinal pathological damage and inflammatory abnormalities were markedly alleviated, accompanied by restoration of gut microbial homeostasis, improved motor performance, and attenuation of the reduction in nigral TH-positive cell density. Together, these results suggest that DZF exerts protective effects across the gut–brain axis by simultaneously improving intestinal microenvironmental disorders and central PD-like pathological changes.

Pathological α Syn transmission from the gut to the brain *via* the vagus nerve is a hallmark event in enterogenic PD (*7-10*). Therefore, we further investigated

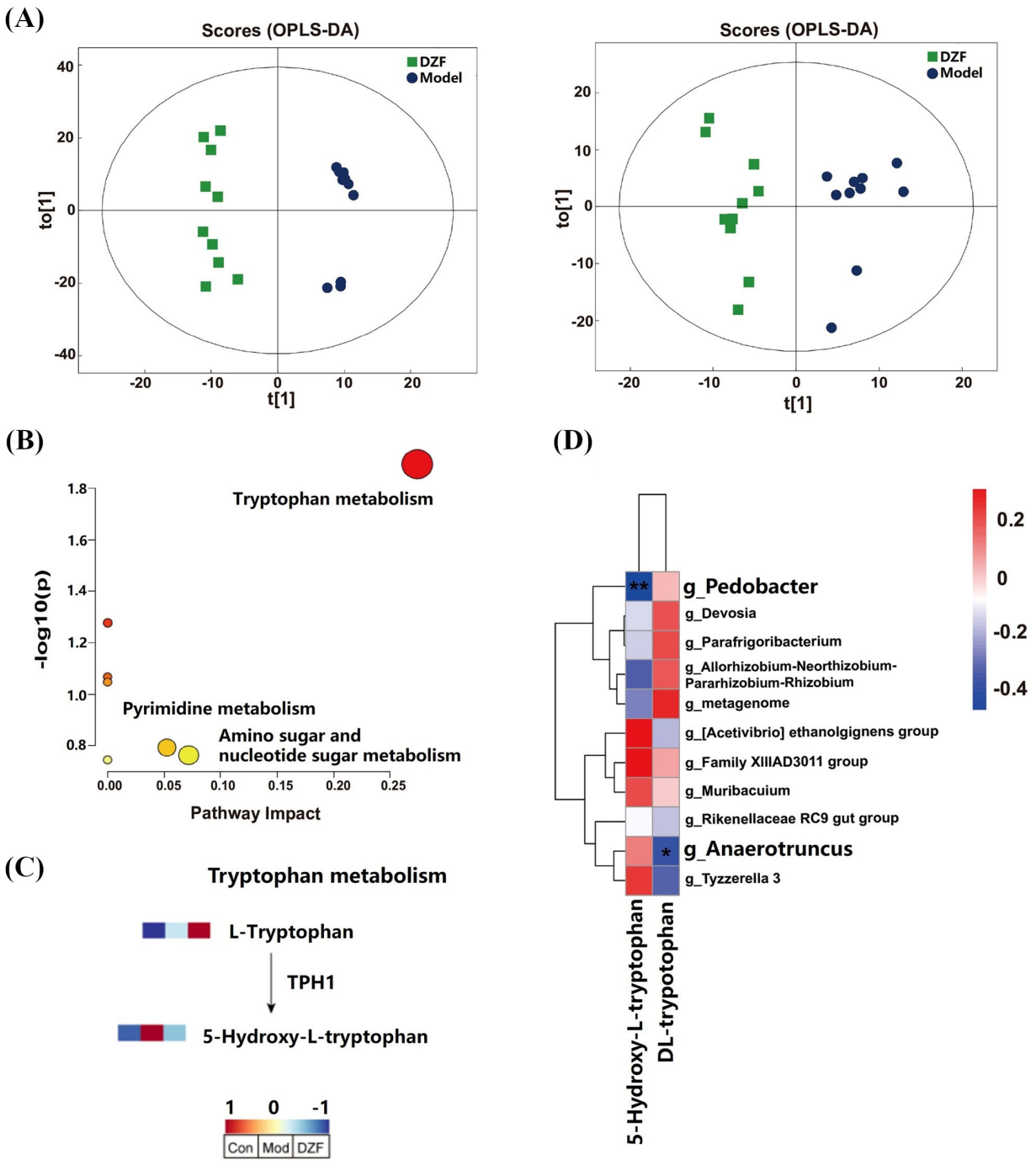

Figure 6. DZF-associated changes in fecal metabolites and tryptophan-related metabolism in PD-like mice. The OPLS-DA score plot (**A**) shows separation between the DZF and model groups. Pathway enrichment analysis (**B**) revealed that tryptophan metabolism was significantly enriched among the altered metabolic pathways and exhibited a relatively high pathway-impact value. The L-tryptophan–TPH1–5-hydroxytryptamine (5-HT) metabolic axis was summarized based on the identified tryptophan-related metabolites (**C**). Spearman correlation analysis shows associations between differential genera and tryptophan-related metabolites, including significant correlations involving *Pedobacter* and *Anaerotruncus* (**D**).

the effect of DZF on α Syn transfer along the gut brain axis to clarify its gut brain mechanistic linkage. In the present study, DZF treatment markedly reduced α-Syn expression in the vagus nerve and brain, while colonic α-Syn levels also showed a decreasing trend following DZF administration. This finding is in full agreement with the Braak hypothesis (*4*) and the study by Kim *et al.* (*9*), who showed that vagotomy completely prevents α Syn propagation to the brainstem. Of note, although colonic α Syn showed a clear decreasing trend in our study, the reduction did not reach statistical significance, possibly due to the small sample size (n = 3). These findings suggest that DZF may alleviate α-Syn-related pathology along the gut–vagus–brain axis, potentially

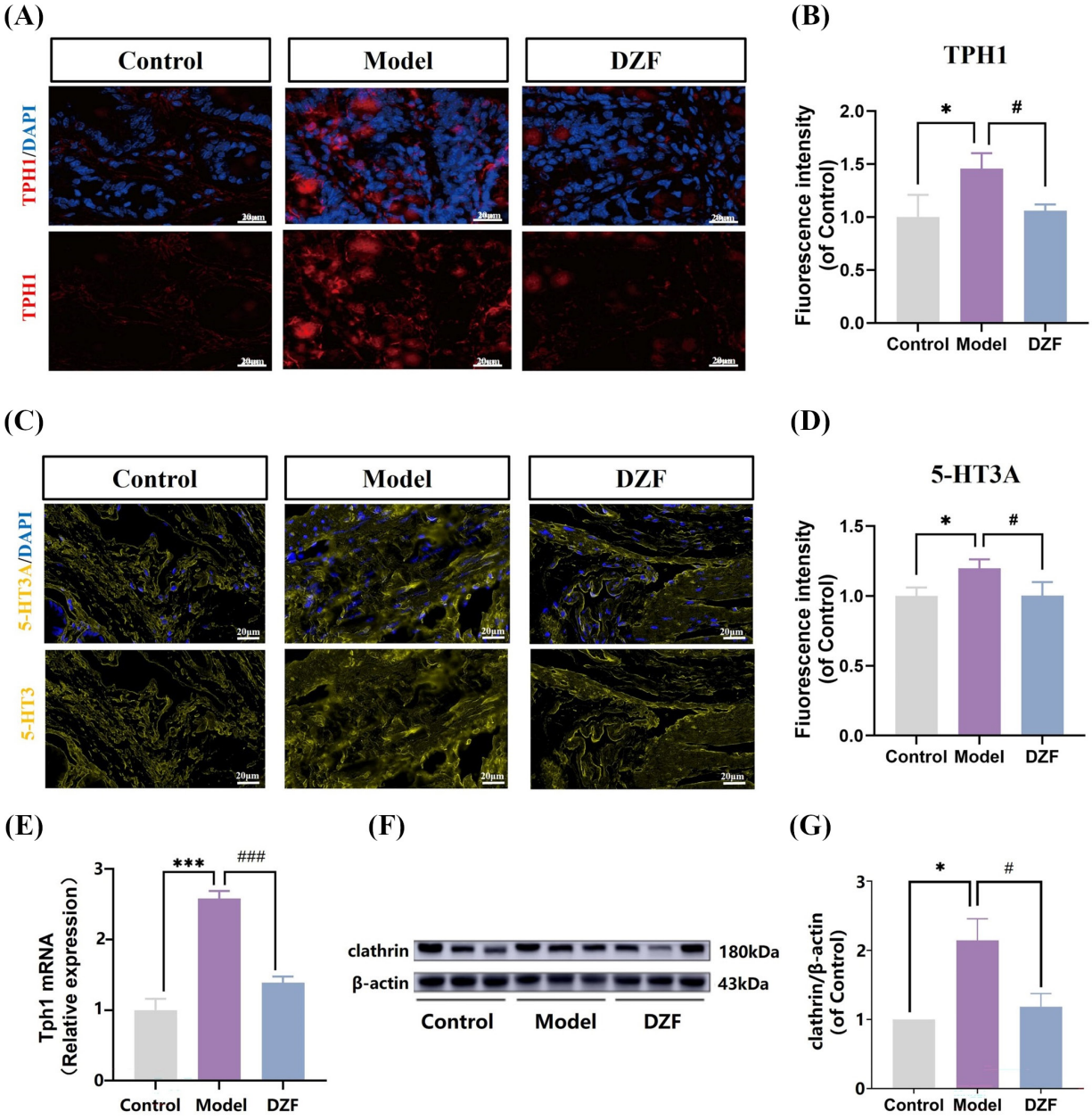

Figure 7. Immunofluorescence staining and quantification showed that rotenone exposure increased TPH1 fluorescence intensity in the colonic epithelium, whereas DZF treatment attenuated this increase (A-B). Similarly, 5-HT3A expression was elevated in the model group and reduced following DZF administration (**C-D**). qPCR analysis further confirmed the changes in intestinal TPH1 mRNA expression after rotenone exposure and DZF treatment (**E**). Western blot analysis showed that DZF treatment decreased the rotenone-induced elevation of Clathrin expression (**F-G**). Data are presented as mean ± SEM, $n = 3$ per group. $^{*}P < 0.05$, $^{**}P < 0.01$ compared with the control group; $^{\#}P < 0.05$, $^{\#\#}P < 0.01$ compared with the model group.

affecting α-Syn accumulation and its associated pathological processes rather than directly demonstrating clearance of established intestinal α-Syn aggregates.

Of interest, untargeted metabolomics analysis revealed that tryptophan metabolism was among the metabolic pathways potentially influenced by DZF intervention. The enrichment analysis identified tryptophan metabolism as a significantly enriched pathway. Consistently, alterations in tryptophan-related metabolites, including L-tryptophan and 5-HTP, further supported the involvement of this pathway in DZF-mediated metabolic regulation. Given that the gut microbiota is considered an important upstream regulator of intestinal tryptophan metabolism (*34*), these findings suggest a potential link between microbiota remodeling and tryptophan-related metabolic changes following DZF treatment. Integrative correlation analysis of microbiome sequencing and metabolomics data showed that specific bacterial genera, particularly *Anaerotruncus* and *Pedobacter*, were significantly correlated with tryptophan-related metabolites, suggesting that DZF-induced microbiota remodeling may be associated with

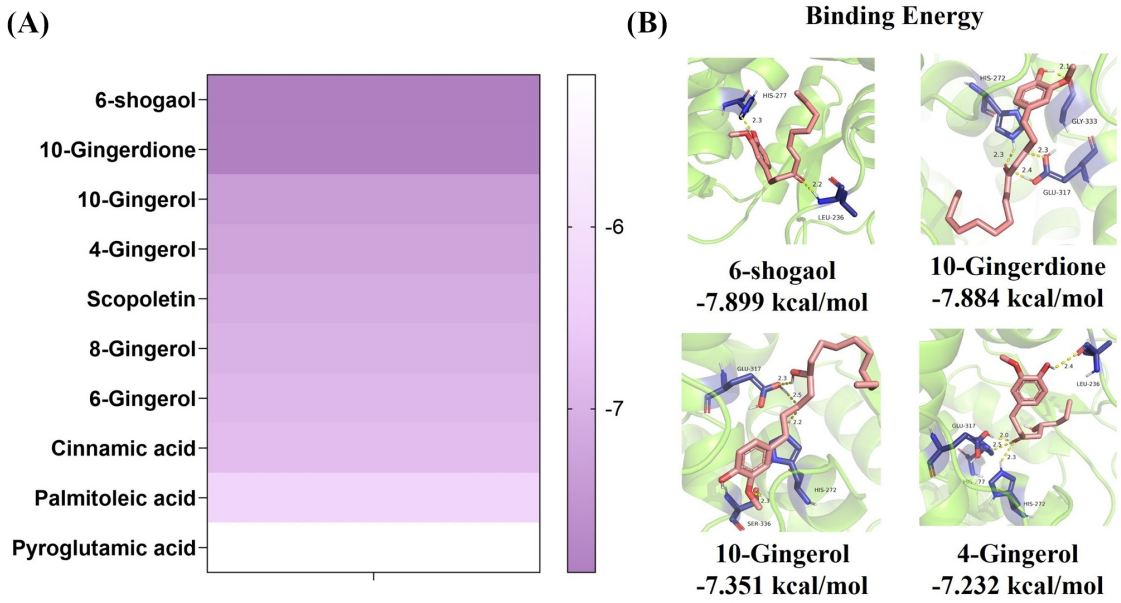

Figure 8. Predicted molecular interactions between intestinal active components of DZF and TPH1. (**A**) Heatmap showing the predicted binding energies of ten intestinal active components of DZF with TPH1 based on molecular docking analysis. (**B**) Representative predicted binding poses of 6-shogaol, 10-gingerdione, 10-gingerol, and 4-gingerol with TPH1.

changes in the intestinal tryptophan metabolic network. Literature reports indicate that *Anaerotruncus* is enriched in the gut of PD patients and is associated with motor and non-motor symptoms (*35*), whereas the functional significance of *Pedobacter* remains to be further explored. These findings suggest that DZF may influence host metabolic regulation through microbiota-associated modulation of tryptophan metabolism.

It has been reported that approximately 95% of peripheral 5 HT is synthesized by intestinal enterochromaffin cells *via* TPH1 (*34,36,37*), and 5 HT is intimately associated with α Syn pathology. Jinsmaa *et al.* found that the 5 HT metabolite 5 hydroxyindole acetaldehyde (5 HIAL) potently promotes α Syn oligomerization; Tripathi *et al.* reported that a 5 HT1b/1d receptor agonist reduces α Syn deposition in the brain of PD rats. Mechanistically, 5 HT promotes Clathrin mediated endocytosis (*38-40*), a key pathway for α Syn entry into neurons. Based on the alterations in L-tryptophan and 5-HTP identified by metabolomics, we further examined intestinal TPH1/5-HT-related signaling. DZF treatment reduced colonic TPH1 protein expression and mRNA levels, accompanied by decreased 5-HT3A expression and attenuation of rotenone-induced Clathrin upregulation (Figure 7). Together, these findings suggest that DZF may modulate intestinal TPH1/5-HT-related signaling and associated intracellular transport processes, thereby contributing to the improvement of gut-derived PD-like pathology. However, because intestinal 5-HT levels and TPH1 enzymatic activity were not directly measured, our findings indicate a potential involvement of TPH1/5-HT-related signaling rather than demonstrating direct regulation of 5-HT synthesis or α-Syn propagation. This suggests that the role of intestinal 5-HT signaling in PD may extend beyond its traditional association with constipation (*41*).

Furthermore, a recent study reported that the antidepressant vortioxetine alleviates rotenone induced intestinal inflammation by enhancing 5 HT signaling (*42*), which appears opposite to the 5 HT suppressing effect of DZF. This apparent contradiction may be explained by the biphasic or context dependent nature of 5 HT signaling: under physiological conditions, appropriate levels of 5 HT help maintain intestinal homeostasis and motor function, whereas in the chronic inflammatory microenvironment of PD, excessive 5 HT may drive α Syn propagation by overactivating endocytosis or promoting immune cell activation. Thus, both enhancing 5 HT (to correct a possible deficiency) and inhibiting 5 HT (to curb excess) may be beneficial under different pathological states. The action of DZF tends to restore 5 HT system homeostasis rather than simply suppressing or activating it. This mechanism still requires further validation in enterochromaffin cell neuron co culture systems.

Previous pharmacokinetic studies have shown that some components of DZF can enter the brain and exert neuroprotective effects. In contrast, other components remain as parent compounds in feces and intestinal contents after administration, exhibiting an "intestinal retention" property (*26*). This phenomenon suggests that these components may exert biological effects through local modulation of intestinal functions. Based on this observation, we further performed molecular docking analysis between these intestinally retained components and TPH1. Several gingerol-like compounds, including 6-shogaol, 10-gingerdione, 10-gingerol, and 4-gingerol, exhibited favorable predicted binding affinities with

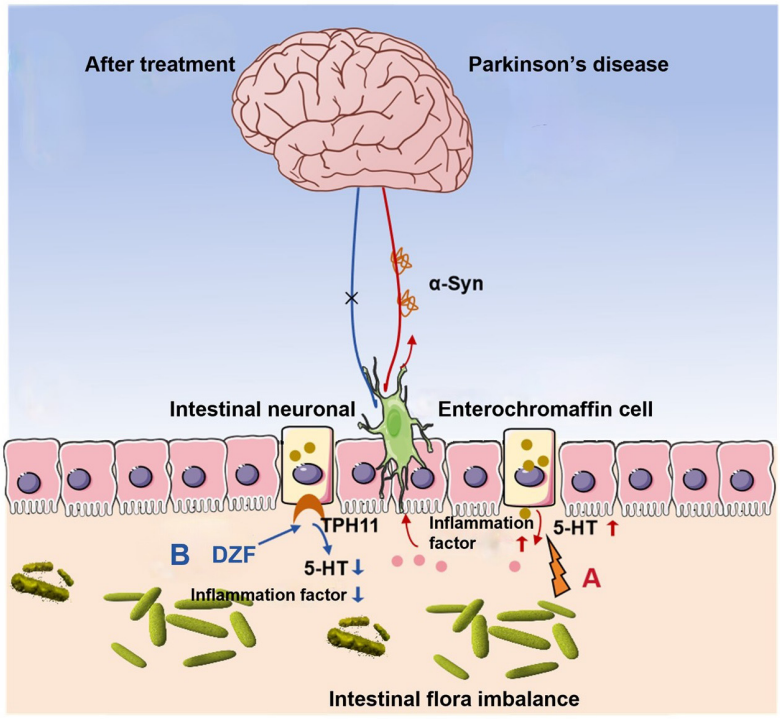

Figure 9. Proposed mechanism underlying the protective effects of DZF against rotenone-induced PD-like pathology through gut-brain axis regulation.

TPH1 (Figure 8). These findings suggest that intestinally retained DZF components may potentially participate in the regulation of TPH1-related signaling and contribute to the intestinal effects of DZF. However, molecular docking analysis alone cannot establish direct binding, TPH1 inhibition, effective intestinal exposure, or therapeutic efficacy. Further biophysical binding assays, enzyme activity measurements, and intestinal pharmacokinetic studies are required to validate these potential interactions.

This study provides evidence that DZF alleviates PD-like pathology through modulation of gut-related abnormalities and TPH1/5-HT-related signaling, while also suggesting a potential role for the gut microbiota–tryptophan metabolism network in its therapeutic effects. However, the precise mechanisms linking intestinal 5-HT-related signaling with α-Syn pathology remain to be further clarified. Future studies involving direct measurement of intestinal 5-HT levels, evaluation of TPH1 enzymatic activity, and functional validation of 5-HT-mediated effects on α-Syn-related processes will help elucidate this mechanism. In addition, the microbiome and metabolomics analyses performed in this study reveal associations rather than causal relationships. Longitudinal studies and interventions such as fecal microbiota transplantation will be valuable for determining whether specific microbial taxa, including *Anaerotruncus* and *Pedobacter*, directly contribute to tryptophan metabolism and DZF-mediated effects. These investigations will further advance our understanding of the gut–brain regulatory mechanisms underlying the protective effects of DZF.

It should be noted that the present study was conducted using a rotenone-induced gut-origin PD mouse model, which reproduces only certain pathological features of human PD and cannot fully recapitulate the complexity of the human disease. Therefore, the neuroprotective effects of DZF require further validation of their efficacy and safety in future clinical studies.

5. Conclusion

In conclusion, this study demonstrates that DZF ameliorates established rotenone-induced PD-like motor dysfunction, intestinal abnormalities, and nigral pathological changes in mice. The findings suggest that intestinally retained DZF components may contribute to these protective effects through modulation of gut microbiota, tryptophan-related metabolism, and TPH1/5-HT-related signaling, accompanied by reduced intestinal inflammation and α-Syn-associated pathology along the gut–brain axis. Molecular docking analysis identified several DZF-derived compounds with potential interactions with TPH1, providing a basis for further investigation of their molecular mechanisms. Overall, this study highlights the potential role of gut-targeted regulation in the protective effects of DZF against PD-like pathology and provides new insights into the gut–brain mechanisms underlying traditional Chinese medicine intervention (Figure 9).

Acknowledgements

The authors would like to express their sincere appreciation to the State Key Laboratory of Component-based Chinese Medicine at Tianjin University of Traditional Chinese Medicine for providing essential experimental platform support. We also thank the technicians at the Animal Experiment Center for their assistance with animal care and behavioral testing. Our gratitude further extends to all members of the research group for their valuable discussions and technical support throughout the study.

Funding: The authors gratefully acknowledge the financial support from the Tianjin Key Program in Traditional Chinese Medicine (Grant No. 2024008) and the Natural Science Foundation of Henan Province (Grant No. 252300420528), which made this study possible.

Conflict of Interest: The authors have no conflicts of interest to disclose.

References

1. Jankovic J, Tan EK. Parkinson's disease: etiopathogenesis and treatment. J Neurol Neurosurg Psychiatry. 2020; 91:795-808.
2. Armstrong MJ, Okun MS. Diagnosis and treatment of Parkinson disease: A review. JAMA. 2020; 323:548-560.
3. Lee JY, Martin-Bastida A, Murueta-Goyena A, Gabilondo I, Cuenca N, Piccini P, Jeon B. Multimodal brain and retinal imaging of dopaminergic degeneration in Parkinson disease. Nat Rev Neurol. 2022; 18:203-220.
4. Braak H, Del Tredici K, Rüb U, de Vos RAI, Jansen Steur ENH, Braak E. Staging of brain pathology related to sporadic Parkinson's disease. Neurobiol Aging. 2003; 24:197-211.
5. Warnecke T, Schäfer KH, Claus I, Del Tredici K, Jost WH. Gastrointestinal involvement in Parkinson's disease: pathophysiology, diagnosis, and management. NPJ Parkinsons Dis. 2022; 8:31.
6. Zhang J, Shi M, Zhang Q, Chen Y, Yin X, Wang X, Zhang Y. Association between constipation and the risk of Parkinson's disease among participants in the UK Biobank. Neuroepidemiology. 2025; 59:381-390.
7. Uemura N, Yagi H, Uemura MT, Hatanaka Y, Yamakado H, Takahashi R. Inoculation of α-synuclein preformed fibrils into the mouse gastrointestinal tract induces Lewy body-like aggregates in the brainstem *via* the vagus nerve. Mol Neurodegener. 2018; 13:21.
8. Holmqvist S, Chutna O, Bousset L, Aldrin-Kirk P, Li W, Björklund T, Wang ZY, Roybon L, Melki R, Li JY. Direct evidence of Parkinson pathology spread from the gastrointestinal tract to the brain in rats. Acta Neuropathol. 2014; 128:805-820.
9. Kim S, Kwon SH, Kam TI, *et al.* Transneuronal propagation of pathologic α-synuclein from the gut to the brain models Parkinson's disease. Neuron. 2019; 103:627-641.e7.
10. Ahn EH, Kang SS, Liu X, Chen G, Zhang Z, Chandrasekharan B, Alam AM, Neish AS, Cao X, Ye K. Initiation of Parkinson's disease from gut to brain by δ-secretase. Cell Res. 2020; 30:70-87.
11. Limanaqi F, Zecchini S, Ogno P, Artusa V, Fenizia C, Saulle I, Vanetti C, Garziano M, Strizzi S, Trabattoni D, Clerici M, Biasin M. Alpha-synuclein shapes monocyte and macrophage cell biology and functions by bridging alterations of autophagy and inflammatory pathways. Front Cell Dev Biol. 2024; 12:1421360.
12. Sampson TR, Debelius JW, Thron T, *et al.* Gut microbiota regulate motor deficits and neuroinflammation in a model of Parkinson's disease. Cell. 2016; 167:1469-1480.e12.
13. Tan AH, Lim SY, Lang AE. The microbiome-gut-brain axis in Parkinson disease: from basic research to the clinic. Nat Rev Neurol. 2022; 18:476-495.
14. Wang L, Cui Y, Han B, Du Y, Salewala KS, Wang S, Zhao W, Zhang H, Wang S, Xu X, Ma J, Zhu Y, Tuo H. Gut microbiota and Parkinson's disease. Chin Med J (Engl). 2025; 138:289-297.
15. Bedarf JR, Hildebrand F, Coelho LP, Sunagawa S, Bahram M, Goeser F, Bork P, Wüllner U. Functional implications of microbial and viral gut metagenome changes in early stage L-DOPA-naïve Parkinson's disease patients. Genome Med. 2017; 9:39.
16. Liang Y, Zhao Y, Fasano A, Su CW. Gut permeability and microbiota in Parkinson's disease: mechanistic insights and experimental therapeutic strategies. Int J Mol Sci. 2025; 26:9593.
17. Radisavljevic N, Metcalfe-Roach A, Cirstea M, Tabusi MM, Bozorgmehr T, Bar-Yoseph H, Finlay BB. Microbiota-mediated effects of Parkinson's disease medications on Parkinsonian non-motor symptoms in male transgenic mice. mSphere. 2024; 9:e0037923.
18. Ramadan ME, Mostafa TM, Ghali AA, El-Afify DR. Randomized controlled trial evaluating synbiotic supplementation as an adjuvant therapy in the treatment of Parkinson's disease. Inflammopharmacology. 2025; 33:3897-3908.
19. Leta V, Zinzalias P, Batzu L, *et al.* Effects of a four-strain probiotic on gut microbiota, inflammation, and symptoms in Parkinson's disease: A randomized clinical trial. Mov Disord. 2025; 40:2710-2721.
20. Wang J, Xue L, Zhang M, Shen P, Zhao W, Tong Q, Wu S, Dai W, Yang X, Wang H. Colonoscopic fecal microbiota transplantation for mild-to-moderate Parkinson's disease: a randomized controlled trial. Brain Behav Immun. 2025; 130:106086.
21. DuPont HL, Suescun J, Jiang ZD, Brown EL, Essigmann HT, Alexander AS, DuPont AW, Iqbal T, Utay NS, Newmark M, Schiess MC. Fecal microbiota transplantation in Parkinson's disease: a randomized repeat-dose, placebo-controlled clinical pilot study. Front Neurol. 2023; 14:1104759.
22. Zhang R, Feng R, Wang J, Chen Y, Liu H, Zhu Q, Tian H, Qin C, Teng J, Tang B, Wu M, Zeng J, Wu E, Ding X, Wang X. Gut microbiota modulation *via* repeated donor fecal transplantation improves motor and gastrointestinal symptoms in drug-naïve Parkinson's disease: a randomized phase 2 trial. Signal Transduct Target Ther. 2026; 11:94.
23. Park JC, Chang L, Kwon HK, Im SH. Beyond the gut: decoding the gut-immune-brain axis in health and disease. Cell Mol Immunol. 2025; 22:1287-1312.
24. Shen Q, Liu RT, Wang Y, Zhuang PW, Yang WH, Guo H. Duzhong Fang ameliorates cognitive impairment of Parkinsonian mice by suppressing neuronal apoptotic pathway. Drug Discov Ther. 2024; 18:229-239.

25. Li L, Fan S, Zhang W, Li D, Yang Z, Zhuang P, Han J, Guo H, Zhang Y. Duzhong Fang attenuates the POMC-derived neuroinflammation in Parkinsonian mice. J Inflamm Res. 2021; 14:3261-3276.
26. Song L, Yin H, Han R, Li J, Ma N, Wang Y, Guo H. Metabolism of Du Zhong Formula in rats using UPLC-Q-TOF/MS. J Mass Spectrom. 2022; 57:e4795.
27. Pan-Montojo F, Anichtchik O, Dening Y, Knels L, Pursche S, Jung R, Jackson S, Gille G, Spillantini MG, Reichmann H, Funk RHW. Progression of Parkinson's disease pathology is reproduced by intragastric administration of rotenone in mice. PLoS One. 2010; 5:e8762.
28. Hajare S, Kulkarni YA. Parkinson's disease and the gut-brain connection: Unveiling pathways, mechanisms and promising therapies. Brain Res. 2025; 1868:149975.
29. Jin X, Wei J, Min X, Fan Y, Yuan Z, Du Z, Su Z, Xun T, Du Q, Liang T, He X, Tang W. Gut microbiota and Parkinson's disease: exploring pathogenesis and potential therapeutic strategies from a gut-brain axis perspective. iScience. 2026; 29:114185.
30. Ratajczyk K, Kaczorowska E, Wyka K, Tarasiuk-Zawadzka A, Fichna J, Gajos A. Gut-brain signaling in Parkinson's disease: a narrative review. Int J Mol Sci. 2026; 27:3531.
31. Klingelhoefer L, Reichmann H. Pathogenesis of Parkinson disease: the gut-brain axis and environmental factors. Nat Rev Neurol. 2015; 11:625-636.
32. Pan-Montojo F, Schwarz M, Winkler C, Arnhold M, O'Sullivan GA, Pal A, Said J, Marsico G, Verbavatz JM, Rodrigo-Angulo M, Gille G, Funk RHW, Reichmann H. Environmental toxins trigger PD-like progression *via* increased alpha-synuclein release from enteric neurons in mice. Sci Rep. 2012; 2:898.
33. Camacho M, Greenland JC, Daruwalla C, Scott KM, Patel B, Apostolopoulos D, Ribeiro J, O'Reilly M, Hu MT, Williams-Gray CH. The profile of gastrointestinal dysfunction in prodromal to late-stage Parkinson's disease. NPJ Parkinsons Dis. 2025; 11:123.
34. Agus A, Planchais J, Sokol H. Gut microbiota regulation of tryptophan metabolism in health and disease. Cell Host Microbe. 2018; 23:716-724.
35. Heintz-Buschart A, Pandey U, Wicke T, Sixel-Döring F, Janzen A, Sittig-Wiegand E, Trenkwalder C, Oertel WH, Mollenhauer B, Wilmes P. The nasal and gut microbiome in Parkinson's disease and idiopathic rapid eye movement sleep behavior disorder. Mov Disord. 2018; 33:88-98.
36. Hummerich R, Schloss P. Serotonin: more than a neurotransmitter: transglutaminase-mediated serotonylation of C6 glioma cells and fibronectin. Neurochem Int. 2010; 57:67-75.
37. Wei L, Singh R, Ghoshal UC. Enterochromaffin cells-gut microbiota crosstalk: underpinning the symptoms, pathogenesis, and pharmacotherapy in disorders of gut-brain interaction. J Neurogastroenterol Motil. 2022; 28:357-375.
38. Jinsmaa Y, Cooney A, Sullivan P, Sharabi Y, Goldstein DS. The serotonin aldehyde, 5-HIAL, oligomerizes alpha-synuclein. Neurosci Lett. 2015; 590:134-137.
39. Tripathi AS, Fatima N, Tripathi P, Tripathi R, Alka, Zaki MEA, Mohapatra L, Yasir M, Maurya RK. Beneficial effect of 5-HT1b/1d agonist on Parkinson's disease by modulating glutamate and reducing deposition of α-synuclein. J Biochem Mol Toxicol. 2024; 38:e23627.
40. Shearer LJ, Petersen NO, Woodside MT. Internalization of α-synuclein oligomers into SH-SY5Y cells. Biophys J. 2021; 120:877-885.
41. Miquel-Rio L, Sarriés-Serrano U, Pavia-Collado R, Meana JJ, Bortolozzi A. The role of α-synuclein in the regulation of serotonin system: physiological and pathological features. Biomedicines. 2023; 11:541.
42. Samur DN, Yıldırım S, Maytalman E, Kalay M, Tanrıöver G, Özbey G. Vortioxetine attenuates rotenone-induced enteric neuroinflammation *via* modulation of the TLR2/S100B/RAGE signaling pathway in a rat model of Parkinson's disease. Neuropharmacology. 2025; 271:110385.

Received June 25, 2025; Revised August 20, 2026; Accepted August 21, 2026.

**Address correspondence to:*
Pengwei Zhuang, First Teaching Hospital of Tianjin University of Traditional Chinese Medicine, Tianjin 300381, China.
E-mail: zhuangpengwei@163.com

Hong Guo, State Key Laboratory of Component-based Chinese Medicine, Tianjin University of Traditional Chinese Medicine, Tianjin, 301617, China.
E-mail: cacti1983@163.com

Released online in J-STAGE as advance publication August 26, 2026.